

Variance of an anisotropic Bose-Einstein condensate

Shachar Klaiman,¹ Raphael Beinke,¹ Lorenz S.

Cederbaum,¹ Alexej I. Streltsov,^{1,2} and Ofir E. Alon^{3,4,*}

¹*Theoretische Chemie, Physikalisch-Chemisches Institut, Universität Heidelberg,
Im Neuenheimer Feld 229, D-69120 Heidelberg, Germany*

²*Institut für Physik, Universität Kassel,
Heinrich-Plett-Str. 40, 34132 Kassel, Germany*

³*Department of Physics, University of Haifa at Oranim, Tivon 36006, Israel*

⁴*Haifa Research Center for Theoretical Physics and Astrophysics,
University of Haifa, Haifa 3498838, Israel*

Abstract

The anisotropy of a trap potential can impact the density and variance of a Bose-Einstein condensate (BEC) in an opposite manner. We exemplify this effect for both the ground state and out-of-equilibrium dynamics of structureless bosons interacting by a long-range inter-particle interaction and trapped in a two-dimensional single-well potential. We demonstrate that even when the density of the BEC is, say, wider along the y direction and narrower along the x direction, its position variance can actually be smaller and momentum variance larger in the y direction than in the x direction. This behavior of the variance in a many-particle system is counterintuitive. It suggests using the variance as a tool to characterize the strength of correlations along the y and x directions in a trapped BEC.

PACS numbers: 03.75.Kk, 67.85.De, 03.75.Hh, 67.85.Bc, 03.65.-w

* ofir@research.haifa.ac.il

I. INTRODUCTION

In quantum mechanics, the variance of an observable $\hat{o}(x)$ for a particle described by the wave-packet $\psi(x)$ is often used to interpret and quantify the physical behavior of the particle [1]. For instance, a wider wave-packet has a larger position variance in comparison with a narrower wave-packet which has a smaller position variance. Physically, the two situations are associated, respectively, with de-localization and localization of the quantum particle. In other words, we are often used to infer the position (and momentum) variance from the shape of the density $|\psi(x)|^2$ of the particle. This intuitive or visual picture may vary in a system made of (many) interacting particles. It is the purpose of this work to demonstrate and investigate such many-body effects using Bose-Einstein condensates as an instrumental example.

Bose-Einstein condensates (BECs) made of ultracold atoms have attracted considerable attention [2–13]. On the theory side, many of the investigations to describe their properties have been performed using Gross-Pitaevskii (mean-field) theory, which assumes all bosons to reside in the same orbital. It is generally perceived that Gross-Pitaevskii theory properly describes the ground state as well as the out-of-equilibrium dynamics of (trapped) BECs in the infinite-particle limit, when the product of the number of particles times the scattering length (i.e., the interaction parameter) is constant. Indeed, there are rigorous results which prove (under certain conditions) that the energy per particle and density per particle of the many-boson system coincide in the infinite-particle limit with the respective Gross-Piteavekii quantities, and that the bosonic system is 100% condensed [14–17], also see in this context [18, 19].

Despite the situation that BECs are 100% in the infinite-particle limit, and that their density per particle and energy per particle coincide with those computed by the Gross-Pitaevskii theory, the story does not end here. In [20, 21] we demonstrated that the variance of a many-particle operator and the uncertainty product of two many-particle operators can substantially deviate from those given by the Gross-Pitaevskii theory, even in the infinite-particle limit when the bosonic system is 100% condensed. Physically, these many-body effects are governed by the (often very small) number of depleted particles which, unlike the non-condensed fraction, does not vanish even in the infinite-particle limit. Mathematically, the difference between the predictions of the many-body and mean-field descriptions can

be tracked down to the subtlety of performing the infinite-particle limit only after (and not before) the many-particle operator is evaluated. In comparison with the variance of an operator of a single particle, the variance of many-particle operators is a much richer quantity, also see [22–25] in this context. At the bottom line, the many-body and mean-field wave-functions themselves differ at the infinite-particle limit and, consequently, their overlap is always smaller than one and can become arbitrarily small [19, 26].

In the present work we would like to investigate the intriguing possibilities which open up for the variance of a trapped BEC in two spatial dimensions, and in particular the connection between shape of the bosonic cloud (i.e., the density) and its position and momentum variance. Intermingled with the above is the investigation of the variance along the pathway from condensation to fragmentation of a trapped BEC. The latter is far away from the infinite-particle limit (where the bosonic system is 100% condensed) which was the focus of previous work [20, 21]. We mention that preliminary results in one spatial dimension were recently reported in [27]. The structure of the paper is as follows. In Sec. II we briefly discuss the variance in a many-body system and its computation from the wave-function of a trapped BEC. In Sec. III we present two detailed investigations, one of the ground state (Subsec. III A) and the second of the out-of-equilibrium dynamics following an interaction quench (Subsec. III B). Conclusions are put forward in Sec. IV. Finally, further details of the numerics and convergence are provided in the Appendix.

II. THEORY

We begin with the many-body Hamiltonian of N interacting bosons

$$\hat{H}(\mathbf{r}_1, \dots, \mathbf{r}_N; \lambda_0) = \sum_{j=1}^N \hat{h}(\mathbf{r}_j) + \sum_{j < k} \lambda_0 \hat{W}(\mathbf{r}_j - \mathbf{r}_k). \quad (1)$$

Here $\hat{h}(\mathbf{r}) = -\frac{1}{2} \frac{\partial^2}{\partial \mathbf{r}^2} + \hat{V}(\mathbf{r})$ is the one-particle Hamiltonian where $V(\mathbf{r})$ the trap potential and $\hat{W}(\mathbf{r}_1 - \mathbf{r}_2)$ the inter-particle interaction of strength λ_0 . Throughout this work $\mathbf{r} = (x, y)$ is the position vector in two spatial dimensions and $\hbar = m = 1$.

In the time-independent part of our work, $\hat{H}(\mathbf{r}_1, \dots, \mathbf{r}_N; \lambda_0) \Phi(\mathbf{r}_1, \dots, \mathbf{r}_N) = E \Phi(\mathbf{r}_1, \dots, \mathbf{r}_N)$, we investigate the ground state of the bosons, where E is the energy and $\Phi(\mathbf{r}_1, \dots, \mathbf{r}_N)$ normalized to unity. In the out-of-equilibrium part we solve the time-dependent Schrödinger equation, $\hat{H}(\mathbf{r}_1, \dots, \mathbf{r}_N; \lambda'_0) \Psi(\mathbf{r}_1, \dots, \mathbf{r}_N; t) = i \frac{\partial \Psi(\mathbf{r}_1, \dots, \mathbf{r}_N; t)}{\partial t}$, for the

scenario where the system evolves following an interaction quench from λ_0 to λ'_0 , with the initial condition $\Psi(\mathbf{r}_1, \dots, \mathbf{r}_N; 0) = \Phi(\mathbf{r}_1, \dots, \mathbf{r}_N)$.

To analyze the many-body wave-function $\Psi(\mathbf{r}_1, \dots, \mathbf{r}_N; t)$ we use its reduced one-body and two-body density matrices [28–31]. The reduced one-body density matrix

$$\begin{aligned} \frac{\rho^{(1)}(\mathbf{r}_1, \mathbf{r}'_1; t)}{N} &= \int d\mathbf{r}_2 \dots d\mathbf{r}_N \Psi^*(\mathbf{r}'_1, \mathbf{r}_2, \dots, \mathbf{r}_N; t) \Psi(\mathbf{r}_1, \mathbf{r}_2, \dots, \mathbf{r}_N; t) = \\ &= \sum_j \frac{n_j(t)}{N} \alpha_j(\mathbf{r}_1; t) \alpha_j^*(\mathbf{r}'_1; t) \end{aligned} \quad (2)$$

is prescribed using the natural orbitals $\alpha_j(\mathbf{r}; t)$ and natural occupations $n_j(t)$. We generally enumerate the occupation numbers in the order of non-increasing values. We call $\sum_{j>1} n_j(t)$ the number of depleted particles (depletion in short) and $\frac{\sum_{j>1} n_j(t)}{N}$ the depleted fraction. The latter are used to define the degree of condensation of the interacting bosons [32]. The diagonal of the reduced one-body density matrix, $\rho(\mathbf{r}; t) = \rho^{(1)}(\mathbf{r}, \mathbf{r}; t)$, is referred to as the density. The diagonal part of the reduced two-body density matrix,

$$\begin{aligned} \frac{\rho^{(2)}(\mathbf{r}_1, \mathbf{r}_2, \mathbf{r}_1, \mathbf{r}_2; t)}{N(N-1)} &= \int d\mathbf{r}_3 \dots d\mathbf{r}_N \Psi^*(\mathbf{r}_1, \mathbf{r}_2, \dots, \mathbf{r}_N; t) \Psi(\mathbf{r}_1, \mathbf{r}_2, \dots, \mathbf{r}_N; t) = \\ &= \sum_{jpkq} \frac{\rho_{jpkq}(t)}{N(N-1)} \alpha_j^*(\mathbf{r}_1; t) \alpha_p^*(\mathbf{r}_2; t) \alpha_k(\mathbf{r}_1; t) \alpha_q(\mathbf{r}_2; t), \end{aligned} \quad (3)$$

is expressed using the natural orbitals, where $\rho_{jpkq}(t) = \langle \Psi(t) | \hat{b}_j^\dagger \hat{b}_p^\dagger \hat{b}_k \hat{b}_q | \Psi(t) \rangle$ and the creation \hat{b}_j (and annihilation) operators are associated with $\alpha_j(\mathbf{r}; t)$.

Using the density per particle and natural orbitals, the variance per particle of an operator $\hat{A} = \sum_{j=1}^N \hat{a}(\mathbf{r}_j)$ which is local in position space reads [20, 21]

$$\begin{aligned} \frac{1}{N} \Delta_{\hat{A}}^2(t) &= \frac{1}{N} \left[\langle \Psi(t) | \hat{A}^2 | \Psi(t) \rangle - \langle \Psi(t) | \hat{A} | \Psi(t) \rangle^2 \right] \equiv \Delta_{\hat{a}, density}^2(t) + \Delta_{\hat{a}, MB}^2(t), \\ \Delta_{\hat{a}, density}^2(t) &= \int d\mathbf{r} \frac{\rho(\mathbf{r}; t)}{N} a^2(\mathbf{r}) - \left[\int d\mathbf{r} \frac{\rho(\mathbf{r}; t)}{N} a(\mathbf{r}) \right]^2, \\ \Delta_{\hat{a}, MB}^2(t) &= \frac{\rho_{1111}(t)}{N} \left[\int d\mathbf{r} |\alpha_1(\mathbf{r}; t)|^2 a(\mathbf{r}) \right]^2 - (N-1) \left[\int d\mathbf{r} \frac{\rho(\mathbf{r}; t)}{N} a(\mathbf{r}) \right]^2 + \\ &+ \sum_{jpkq \neq 1111} \frac{\rho_{jpkq}(t)}{N} \left[\int d\mathbf{r} \alpha_j^*(\mathbf{r}; t) \alpha_k(\mathbf{r}; t) a(\mathbf{r}) \right] \left[\int d\mathbf{r} \alpha_p^*(\mathbf{r}; t) \alpha_q(\mathbf{r}; t) a(\mathbf{r}) \right]. \end{aligned} \quad (4)$$

The first term, $\Delta_{\hat{a}, density}^2(t)$, describes the variance of $\hat{a}(\mathbf{r})$ resulting from the density per particle $\frac{\rho(\mathbf{r}; t)}{N}$. The second term, $\Delta_{\hat{a}, MB}^2(t)$, collects all other contributions to the many-particle variance. $\Delta_{\hat{a}, MB}^2(t)$ is generally non-zero within a many-body theory, but is identically equal to zero within Gross-Pitaevskii theory. We remark that analogous expressions hold for operators which are local in momentum space.

III. RESULTS

Our system of choice is made of structureless bosons with harmonic inter-particle interaction trapped in a single-well *anharmonic* potential. Unlike models of particles interacting with harmonic inter-particle interaction and trapped in a harmonic trap, which have been extensively studied and can be solved analytically [33–47], the Schrödinger equation of the trapped BEC has no analytical solution in the present study, nor even the variance can be determined analytically, thus necessitating a numerical treatment.

For this, we have to employ a suitable many-body theoretical and computational approach. Such a many-body tool is the multiconfigurational time-dependent Hartree (MCTDH) for bosons (MCTDHB) method [48, 49] which has been extensively used in the literature [50–67]. For further documentation of MCTDHB see [68–70], and for its benchmarks with an exactly-solvable model [71] (and [72]). MCTDHB can be seen as the indistinguishable-particle bosonic daughter of MCTDH [73–76].

A. Statics

We investigate the variance along the pathway from condensation to fragmentation of the ground state of trapped bosons [77–81]. Fragmentation of BECs has drawn much attention, see, e.g., [82–90]. In particular for structureless bosons with a long-range interaction in a single trap, the ground state has been shown to become fragmented when increasing the inter-particle repulsion [58, 91–95]. Figs. 1, 2, and 3 below collect the results.

The one-body Hamiltonian in (1) is $\hat{h}(x, y) = -\left(\frac{1}{2}\frac{\partial^2}{\partial x^2} + \frac{1}{2}\frac{\partial^2}{\partial y^2}\right) + \frac{\{x^2 + [(1-\beta)y]^2\}^2}{4}$, where the degree of anisotropy is β . The inter-particle interaction is harmonic and repulsive, $\lambda_0 \hat{W}(x_1 - x_2, y_1 - y_2) = -\lambda_0[(x_1 - x_2)^2 + (y_1 - y_2)^2]$, $\lambda_0 > 0$. Fig. 1 depicts snapshots of the density per particle of $N = 10$ bosons for three interaction strengths $\lambda_0 = 0.01, 0.10$, and 0.20 [the interaction parameters are $\Lambda = \lambda_0(N - 1) = 0.09, 0.9$, and 1.8 , respectively] and three degrees of anisotropy $\beta = 0\%$ (isotropic), 10% , and 20% . We follow the changes in the ground state. The density broadens as the interaction is increased. For the isotropic trap, see the upper row Fig. 1a,b,c, the density remains, of course, rotationally symmetric and eventually a torus-like shape emerges. For the anisotropic traps, the density splits into two clouds, see the middle row Fig. 1d,e,f and lower row Fig. 1g,h,i. The more anisotropic

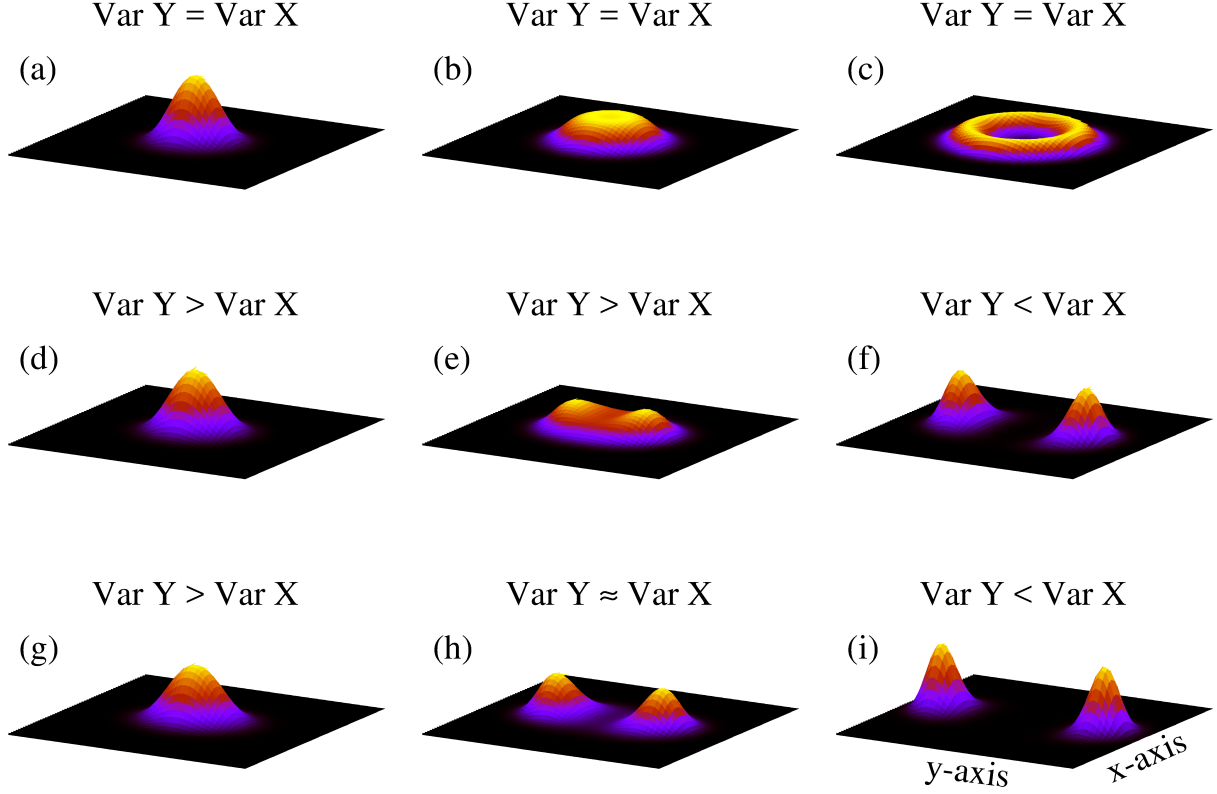


FIG. 1. (Color online) Anisotropy of the variance in the ground state. Shown is the density per particle of $N = 10$ bosons for the interaction strengths $\lambda_0 = 0.01, 0.10$, and 0.20 (left to right columns) and trap anisotropies $\beta = 0\%$ (isotropic), 10% , and 20% (upper to lower rows). Increasing the interaction strength the ground state changes its shape and the reduced one-body density matrix fragments, see Fig. 2. In the upper row, panels (a), (b), and (c), the system is isotropic and naturally the position variances in the y and x directions are equal. In the middle row, panels (d), (e), and (f), and lower row, panels (g), (h), and (i), the system is anisotropic and, as the density in the y direction becomes wider than the density in the x direction, the respective variances surprisingly behave in an opposite manner. That is, the variance in the y direction becomes smaller than that in the x direction, see Fig. 3. This many-body phenomenon, where the anisotropy of the position variance behaves in an opposite manner to the anisotropy of the density, is hence counterintuitive. The results are obtained for $M = 10$ time-adaptive (self-consistent) orbitals. See the text for further discussion. The quantities shown are dimensionless.

is the trap, the more split is the ground-state density for a given interaction parameter.

Along side the changes in the shape of the ground-state density, the reduced one-particle density of the ground state fragments [58, 91–95]. Depending on the anisotropy of the trap and strength of the interaction, the ground state evolves from nearly fully condensed, for $\lambda_0 = 0.01$ and $\beta = 0\%$, to almost fully two-fold fragmented, for $\lambda_0 = 0.20$ and $\beta = 20\%$, see Fig. 2 and discussion below. The more anisotropic is the trap, the more fragmented is the ground state for a given interaction parameter. It is interesting to follow the ‘correlation diagram’ of the occupation numbers [see (2)] for $\lambda_0 = 0.20$. Degenerate occupation numbers for the isotropic trap (n_2, n_3 and n_4, n_5 for $\beta = 0\%$) split when the anisotropy sets in, and together with the non-degenerate occupation numbers (n_1 and n_6 for $\beta = 0\%$) essentially merge to pairs (n_1, n_2 and n_3, n_4 and n_5, n_6 for $\beta = 20\%$) when the fragmentation is full, see Fig. 2.

We now move to the central quantity of interest – the variance. Fig. 3 depicts the many-particle position variance per particle, $\frac{1}{N}\Delta_X^2$, and momentum variance, $\frac{1}{N}\Delta_P^2$, of the ground state for the interaction strengths $\lambda_0 = 0.01, 0.10$, and 0.20 and anisotropies of the trap $\beta = 0\%, 10\%$, and 20% discussed above. Generally, enlarging the anisotropy of the trap (in our case along the y-axis) enlarges the area available for the trapped interacting bosons. For the weakest interaction, $\lambda_0 = 0.01$, the position variance along the y-axis increases monotonically, and that along the x-axis hardly changes, see the upper two curves in Fig. 3a. Side by side, the momentum variance along the y-axis decreases monotonically, whereas that along the x-axis decreases very mildly, see the lower two curves in Fig. 3b. These are compatible with the shapes of the density, see the left column Fig. 1a,d,g, and with the occupation numbers, see Fig. 2, indicating that the systems are essentially fully condensed [$\frac{n_1}{N} > 0.99(9)$ for all three anisotropies].

Already for $\lambda_0 = 0.10$, changing the anisotropy of the trap leads to a different behavior of the variance. At 10% anisotropy, where the system is somewhat depleted with $\frac{n_1}{N} > 0.92$, the position variance along the y-axis slightly increases and that along the x-axis slightly decreases. Accidentally, the momentum variance along both directions are approximately equal (and slightly increase). At 20% anisotropy the position variance along both directions are incidentally approximately equal (and decrease), and the momentum variance along the y-axis is larger than that along the x-axis (both increase). The system is now already two-fold fragmented with $\frac{n_1}{N} = 0.73$ and $\frac{n_2}{N} = 0.26$. Looking at the shapes of the density in

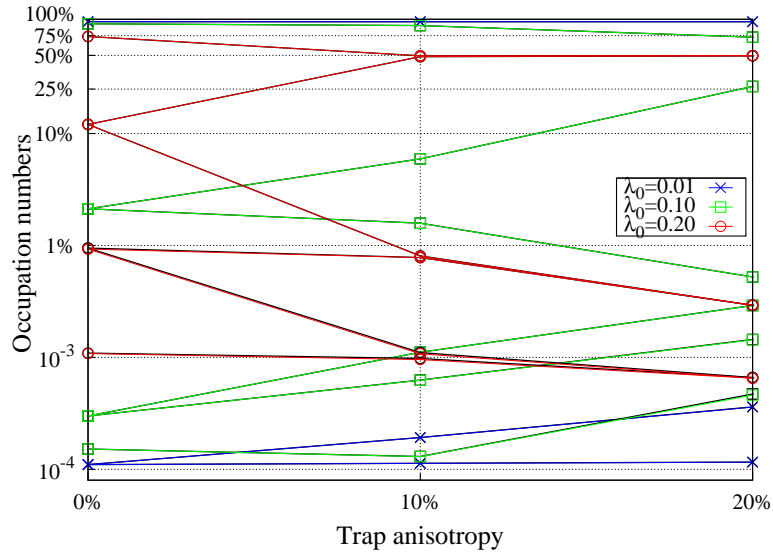


FIG. 2. (Color online) Occupation numbers n_j/N for $N = 10$ bosons with interactions of different strengths, and in traps of different anisotropies, throughout the pathway from condensation to fragmentation of the ground state. The three largest occupation numbers for $\lambda_0 = 0.01$ (blue curves with stars) computed with $M = 3$ time-adaptive (self-consistent) orbitals and the six largest occupations numbers for $\lambda_0 = 0.10$ (green curves with boxes) and $\lambda_0 = 0.20$ (red curves with circles) computed with $M = 10$ orbitals (actual data are marked by symbols, the curves are to guide the eye). Fragmentation of the ground state with increasing interaction strength and anisotropy of the trap is demonstrated, see the text for further discussion. Also plotted by the black curves with the same palette of symbols are the results obtained by including the next ‘filled shell’ of orbitals, namely, $M = 6$ and $M = 15$, respectively. It is seen that the results with $M = 3$ and $M = 6$ orbitals for the weakest interaction, and the results with $M = 10$ and $M = 15$ orbitals for the stronger interactions lie atop each other. The quantities shown are dimensionless.

the middle column Fig. 1b,e,h, we observe the effects of the depletion and more visibly of the fragmentation on the variance. The many-body term of the variance becomes dominant over the density term of the variance [see (4)] in the ground state of the system.

The results for $\lambda_0 = 0.20$ are even more prominent. First, despite the fact that the density broadens along the y -axis while the anisotropy is enlarged, the position variance decreases (in both directions, but more mildly in the x direction). Moreover and in an opposite manner, the y -axis position variance is smaller than that along the x -axis, see lower two curves in Fig. 3a, although the density along the y -axis is much broader than that along the x -axis, see the right column Fig. 1c,f,i. The behavior of the momentum variance is in line with the above many-body effects. The momentum variance along the y -axis is

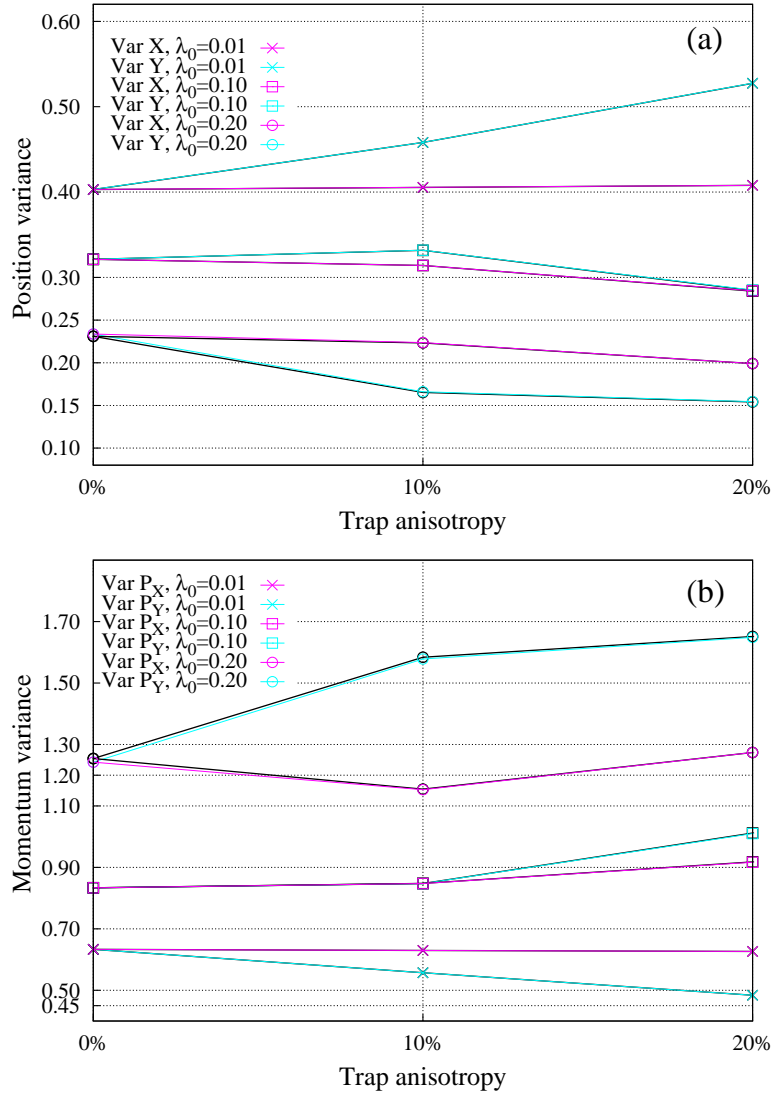


FIG. 3. (Color online) (a) Position variance per particle $\frac{1}{N}\Delta_X^2$ and $\frac{1}{N}\Delta_Y^2$ and (b) momentum variance $\frac{1}{N}\Delta_{\hat{P}_X}^2$ and $\frac{1}{N}\Delta_{\hat{P}_Y}^2$ for $N = 10$ bosons in traps of different anisotropies and for interactions of different strengths throughout the pathway from condensation to fragmentation of the ground state. The magenta curves and symbols are for quantities along the x direction and the cyan curves and symbols are for quantities along the y direction (actual data are marked by symbols, the curves are to guide the eye). Crosses are data for $\lambda_0 = 0.01$ (computed with $M = 3$ orbitals), and boxes are for $\lambda_0 = 0.10$ and circles for $\lambda_0 = 0.20$ (computed with $M = 10$ orbitals). Anisotropy of the variance is demonstrated, see the text and Fig. 1 for further discussion. Also plotted by the black curves with the same palette of symbols are the results obtained by including the next ‘filled shell’ of orbitals, namely, $M = 6$ and $M = 15$, respectively. It is seen that the results with $M = 3$ and $M = 6$ orbitals for the weakest interactions, and the results with $M = 10$ and $M = 15$ orbitals for the stronger interactions practically lie atop each other. The quantities shown are dimensionless.

larger than that along the x -axis, i.e., opposite to the shape of the density. Furthermore, the momentum variance increases monotonously along the y direction, but first decreases and then increases along the x direction. The occupation numbers, $\frac{n_1}{N} = 0.49(5)$ and $\frac{n_2}{N} = 0.49$ for $\beta = 10\%$ and $\frac{n_1}{N} \approx 0.5$ and $\frac{n_2}{N} \approx 0.5$ for $\beta = 20\%$, signify that the system becomes essentially fully two-fold fragmented. Again and more pronouncedly, the many-body term of the variance is dominant over the density term of the variance [see (4)] when the ground state is fragmented.

Let us recapitulate. As a two-dimensional isotropic anharmonic trap is stretched along the y direction, the density basically broadens in that direction. The long-range interaction causes the system to fragment. Then, the position variance decreases and the momentum variance increases, unlike from what one could anticipate by just examining the shape of the density. On top of that, we find that, although the density of the cloud is anisotropic, here it is broader along the y -axis than along the x -axis, the position variance along the y direction is smaller than that along the x direction. Correspondingly, the momentum variance along the y direction is larger than that along the x direction. We stress that this is contrary to what one would expect by just examining the shape of the two-dimensional density. All in all, these are intriguing many-body effects in the ground state of a fragmented trapped BEC.

B. Dynamics

The counter-intuitive properties of the position and momentum variances discussed in Subsec. III A are associated with the larger depleted fraction and more pronounced fragmentation of the ground state of a finite Bose system. The natural question to ask is whether such or similar effects can occur in larger systems. In the present subsection we shall demonstrate that the answer is positive and concentrate on an out-of-equilibrium scenario. We thereby keep in mind that we are *en route* the limit of an infinite number of particles where the depletion per particle of the system diminishes to zero.

The one-body Hamiltonian is again $\hat{h}(x, y) = -\left(\frac{1}{2}\frac{\partial^2}{\partial x^2} + \frac{1}{2}\frac{\partial^2}{\partial y^2}\right) + \frac{\{x^2 + [(1-\beta)y]^2\}^2}{4}$, where the degree of anisotropy is $\beta = 0\%$, 10% , and 20% , and the inter-particle interaction is harmonic and repulsive, $\lambda_0 \hat{W}(x_1 - x_2, y_1 - y_2) = -\lambda_0[(x_1 - x_2)^2 + (y_1 - y_2)^2]$, $\lambda_0 > 0$. We consider the smallest interaction parameter from the above ground-state study, $\Lambda = \lambda_0(N - 1) = 0.09$,

but take a hundred times larger number of interacting bosons, $N = 1000$. The system is prepared in the ground state of the trap. The initial depletion fraction is accordingly a hundred times smaller [$\frac{n_1(0)}{N} > 0.9999(9)$] for each of the three anisotropies $\beta = 0\%$, 10% , and 20% than for the corresponding cases with $N = 10$ bosons in Subsec. III A. The initial densities per particle look just like the left column Fig. 1a,d,g.

At $t = 0$ the interaction parameter is suddenly quenched to twice its value $\Lambda' = \lambda'_0(N - 1) = 0.18$. We ask what the out-of-equilibrium dynamics of the system would be like. Figs. 4 and 5 collect the results. A complementary and comparative investigation for $N = 10$ bosons and the same interaction-quench scenario is presented in the Appendix.

Following the quench of the interaction, the density performs breathing oscillations [94, 96, 97], i.e., its widths along the y and x directions varies in time. Furthermore, since the interaction is repulsive and at $t = 0$ suddenly increased, the density first expands at short times, i.e., the cloud initially broadens both along the y and x directions.

We have performed the calculations of the out-of-equilibrium dynamics both at the Gross-Pitaevskii level ($M = 1$) and at the many-body level ($M = 3$). The two-dimensional time-dependent many-body density per particle, $\frac{\rho(\mathbf{r};t)}{N}$, essentially coincides with the corresponding mean-field density. This is quite reasonable and expected due to the initial marginal depletion fraction [$\frac{n_1(0)}{N} > 0.9999(9)$] which remains very small throughout the evolution of the BEC in time, see below. As far as the condensed fraction is considered, the system remains essentially fully condensed, also see [21, 27] for respective out-of-equilibrium studies in a one-dimensional trap.

In Fig. 4 the time-dependent many-particle position variance per particle, $\frac{1}{N}\Delta_X^2(t)$ [panels (a), (b), and (c)], and momentum variance, $\frac{1}{N}\Delta_P^2(t)$ [panels (d), (e), and (f)], are shown. The many-body and mean-field results are compared for each of the three trap anisotropies $\beta = 0\%$, 10% , and 20% . In Fig. 5 the total number of depleted particles outside the condensed mode [$\alpha_1(\mathbf{r};t)$ natural orbital] are shown as a function of time. The systems are essentially fully condensed with only a fraction of a single particle being depleted.

We start by analyzing the out-of-equilibrium dynamics in the isotropic trap, see Fig. 4a,d. The results and discussion are to assist one in analyzing the dynamics in the anisotropic traps. For the isotropic trap, the quantities along the y and x directions, of course, coincide. Both the many-body and mean-field variances vary in time in an oscillatory manner. However, there are a couple of clearly visible differences. The first, is that the mean-field variances

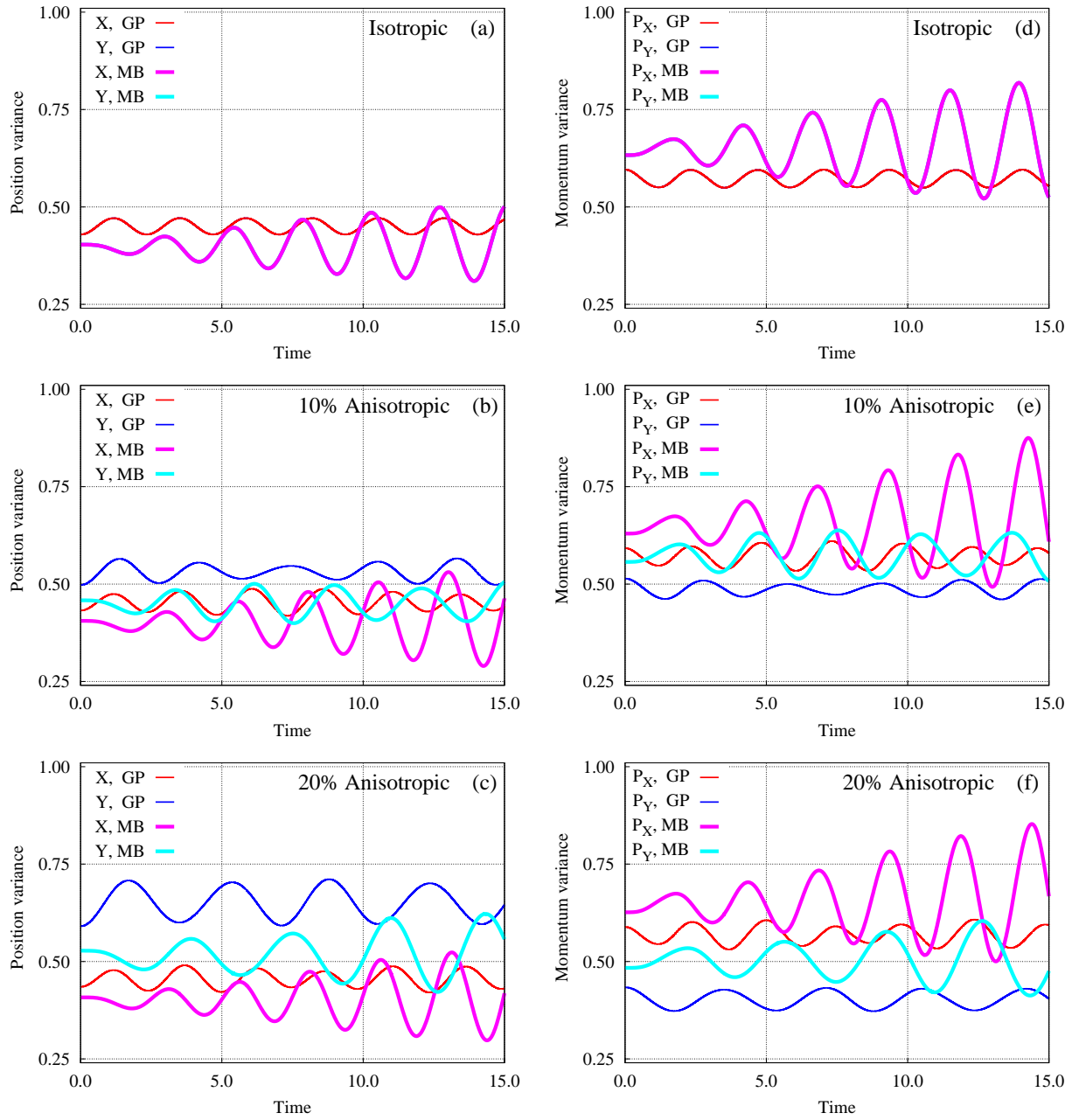


FIG. 4. (Color online) Anisotropy in the breathing dynamics following an interaction quench. Shown and compared are the many-body results for $N = 1000$ bosons using $M = 3$ time-adaptive orbitals and the mean-field results (equivalent to $M = 1$). (a),(b),(c) The time-dependent many-particle position variance per particle, $\frac{1}{N}\Delta_X^2(t)$ and $\frac{1}{N}\Delta_Y^2(t)$, and (d),(e),(f) the momentum variance, $\frac{1}{N}\Delta_{P_X}^2(t)$ and $\frac{1}{N}\Delta_{P_Y}^2(t)$, following an interaction quench from $\Lambda = \lambda_0(N - 1) = 0.09$ to 0.18 at $t = 0$ are plotted. For the isotropic system, panels (a),(d), the quantities along the y and x directions are, of course, equal. For the anisotropic systems, panels (b),(e) and (c),(f), the time-dependent position variance in the y and x directions do not cross each other at the mean-field level, and similarly the momentum quantities, signifying that the position (momentum) density in the y direction is always wider (narrower) than that in the x direction. This, however, is no longer the case at the many-body level: A system whose position (momentum) density along the y direction is wider (narrower) than that along the x direction can actually have a smaller (larger)

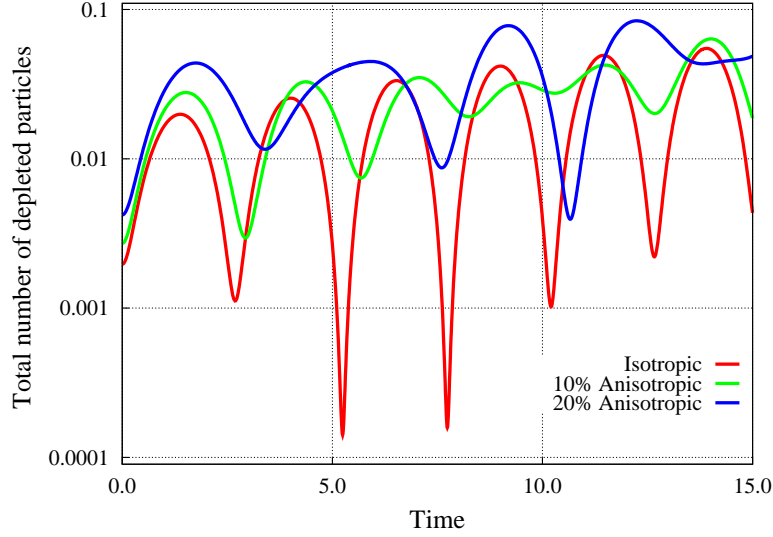


FIG. 5. (Color online) Depletion in the breathing dynamics following an interaction quench. Shown is the total number of depleted particles outside the condensed mode of $N = 1000$ bosons, computed with $M = 3$ time-adaptive orbitals, in the out-of-equilibrium dynamics of Fig. 4. Note the values on the y-axis. See the text for further discussion. The quantities shown are dimensionless.

oscillate with a rather constant amplitude, whereas the many-body variances oscillates with a (slowly) growing amplitude. The latter can be attributed to the (slowly) growing amount of depleted particles, see Fig. 5, albeit less than one tenth of a particle is outside the condensed mode! Indeed, the variance is a highly sensitive probe of correlations even when the system is practically condensed [20, 21]. The second difference, is the opposite dynamical behavior of the variances at short times when computed at the many-body and Gross-Pitaevskii levels. Despite the expansion of the cloud at short times, the time-dependent position variance increases and momentum variance decreases, implying that the many-body contributions to the variance $\Delta_{\hat{x},MB}^2(t) = \Delta_{\hat{y},MB}^2(t)$ and $\Delta_{\hat{p}_x,MB}^2(t) = \Delta_{\hat{p}_y,MB}^2(t)$ are opposite in sign with respect to and dominate the mean-field terms $\Delta_{\hat{x},density}^2(t) = \Delta_{\hat{y},density}^2(t)$ and $\Delta_{\hat{p}_x,density}^2(t) = \Delta_{\hat{p}_y,density}^2(t)$. This is an appealing time-dependent many-body effect taking place in macroscopic Bose systems.

We now turn to the anisotropy of the variance in the y and x directions during the breathing dynamics, see Fig. 4b,c,e,f. When the trap becomes anisotropic, the time-dependent quantities along the y direction ‘split’ from the quantities along the x direction. Since the

isotropic trap is made anisotropic by a stretch along the y -axis, the ‘base line’ of the position variance along the y direction is shifted up to higher values, and the ‘base line’ of the momentum variance along the y axis is shifted down to lower values, at least as far as the (initial conditions and) short-time dynamics is concerned. Obviously, this shift is larger for 20% anisotropy than for 10% anisotropy, compare Fig. 4b,e and Fig. 4c,f. All in all, one can anticipate from (the geometry of the trap and) the shape of the density the anisotropy of the time-dependent position and momentum variances, at least for short times. This result extends what is found in Subsec. III A for the ground-state of an essentially fully-condensed system.

But the geometrical picture of the anisotropy of the variance emerging at short times changes in time. At the mean-field level, the position variances in the y and x directions (which are different in the anisotropic trap) oscillate with a rather constant amplitude. Consequently, they do not cross each other, indicating that during the breathing dynamics the cloud’s density remains wider along the y direction than along the x direction. The corresponding momentum variances also oscillate with a rather constant amplitude and, therefore, do not cross each other as well. This implies that during the dynamics the momentum density of the cloud stays narrower along the y direction than along the x direction.

At the many-body level, on the other hand, the variances along the y and x directions oscillate with a (slowly) growing amplitudes. Therefore, at a certain point in time the y and x position variances must cross each other for the first time. Similarly, the y and x momentum variances must also cross at some point in time. The smaller the anisotropy, the earlier is this time, compare Fig. 4b,e for $\beta = 10\%$ and Fig. 4c,f for $\beta = 20\%$. Thus, the presence of even the slightest time-dependent depletion leads to a large influence on the time-dependent variance at the many-body level: The anisotropy of the variance for a whole time intervals is opposite to the anisotropy of the density. Then, a simple analysis shows that $\Delta_{\hat{x},MB}^2(t) - \Delta_{\hat{y},MB}^2(t) > \Delta_{\hat{y},density}^2(t) - \Delta_{\hat{x},density}^2(t) > 0$ and $\Delta_{\hat{p}_y,MB}^2(t) - \Delta_{\hat{p}_x,MB}^2(t) > \Delta_{\hat{p}_x,density}^2(t) - \Delta_{\hat{p}_y,density}^2(t) > 0$.

We have repeated the investigation of the out-of-equilibrium scenarios for a system of $N = 10$ bosons and the same interaction parameters. The results are collected in the Appendix, see Fig. 6 and 7. The similarity of the out-of-equilibrium results for the same interaction parameter and different numbers of particles ($N = 1000$ bosons in the present

subsection, $N = 10$ in the Appendix), together with analogous behavior in the dynamics of larger systems in one-dimensional traps [21, 27], provide, in our opinion, strong evidences that the effects of the anisotropy of the time-dependent position and momentum variances in essentially fully-condensed BECs persist in the limit of an infinite number of particle.

All in all, we have discussed two out-of-equilibrium effects associated with the variance during the breathing dynamics of essentially-condensed trapped bosons. At short times, it is the decrease (increase) of the position (momentum) variance in contrast to the increase (decrease) of the width of the position (momentum) density. At longer times, it is the opposite behavior of the anisotropy of the variances in position and momentum spaces when computed at the mean-field and many-body levels.

IV. CONCLUSIONS

We have investigated in the present work the variance of the position and momentum many-particle operators of structureless bosons interacting by a long-range inter-particle interaction and trapped in a two-dimensional single-well anharmonic potential. In the first investigation, that of the pathway from condensation to fragmentation of the ground state, we find out that, although the density of the cloud is broader along the y-axis than along the x-axis, the position variance can behave in an opposite manner, namely, be larger along the x-axis than along the y-axis. Similarly, the momentum variance can be larger along the y-axis than along the x-axis. This opposite anisotropy of the variance with respect to the density is a counterintuitive many-body effect that emerges when the ground-state of the bosonic system is fragmented.

In the second study, that of the out-of-equilibrium breathing dynamics of a BEC, we find out that, already when a fraction (even a tenth) of a boson is depleted, qualitative differences between the many-body and mean-field variances arise. Explicitly, the time-dependent many-body position variance can show opposite behavior of the anisotropy between the y-axis and x-axis with respect to the mean-field quantities, despite the system being essentially fully condensed. Corresponding results hold for the time-dependent many-body momentum variance in comparison with the mean-field quantities.

Both the ground-state and out-of-equilibrium scenarios suggest a wealth of effects emanating from the many-body term of the variance both in position and momentum spaces in

interacting trapped many-boson systems, in two spatial dimensions. The anisotropy of the variance advocates that it can be used to characterize the strength of correlations along the y and x directions in the system. We have seen that such many-body effects encoded within the variance do not necessarily match with the information that can be extracted based on the shape of system’s density. This is in sharp contrast to the text-book example of a single particle discussed in the introduction.

ACKNOWLEDGEMENTS

This paper is dedicated to Professor Hans-Dieter Meyer, a dear colleague and friend, on the occasion of his 70th birthday. This research was supported by the Israel Science Foundation (Grant No. 600/15). Partial financial support by the Deutsche Forschungsgemeinschaft (DFG) is acknowledged. We thank Kaspar Sakmann for discussions. Computation time on the Cray XC40 system Hazelhen at the High Performance Computing Center Stuttgart (HLRS) is gratefully acknowledged.

Appendix A: Further computational details and convergence

The multiconfigurational time-dependent Hartree for bosons (MCTDHB) method [48, 49, 68–70, 76] is used in the present work to compute the ground-state and out-of-equilibrium properties of trapped bosons in two spatial dimensions interacting by a long-range inter-particle interaction. The maximal configurational space are 501×501 for $N = 1000$ bosons and $M = 3$ orbitals and $1\,961\,256$ for $N = 10$ bosons and $M = 15$ orbitals. We use the numerical implementation in the software packages [98, 99]. To obtain the ground state we propagate the MCTDHB equations of motion in imaginary time [71, 81]. For the computations the many-body Hamiltonian is represented by 128^2 exponential discrete-variable-representation grid points (using a Fast-Fourier Transform routine) in a box of size $[-10, 10] \times [-10, 10]$. Convergence of the occupation numbers (depletion) and the position and momentum variance with increasing number of ‘filled shells’, namely, $M = 3, 6, 10$, and 15 time-adaptive orbitals, is demonstrated for $N = 10$ bosons in Figs. 2 and 3 for the ground state [20] and in Figs. 6 and 7 for the out-of-equilibrium breathing dynamics [21],

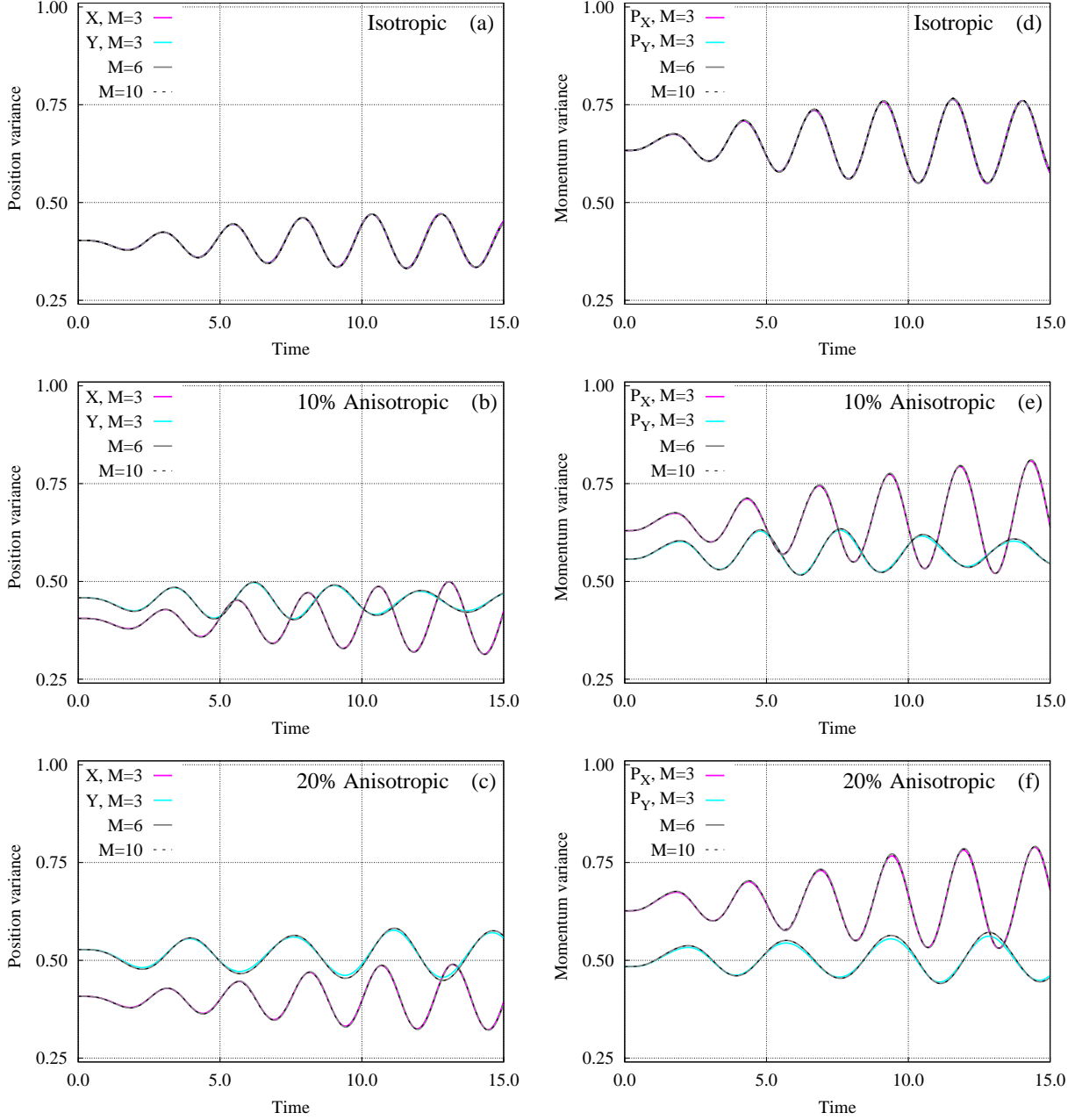


FIG. 6. (Color online) Convergence of the time-dependent many-particle position variance per particle, $\frac{1}{N}\Delta_X^2(t)$ and $\frac{1}{N}\Delta_Y^2(t)$ [panels (a), (b), and (c)], and the momentum variance, $\frac{1}{N}\Delta_{P_X}^2(t)$ and $\frac{1}{N}\Delta_{P_Y}^2(t)$ [panels (d), (e), and (d)], with the number of time-adaptive orbitals M used in the MCTDHB computations for systems consisting of $N = 10$ bosons in traps of anisotropies $\beta = 0\%$, 10% , and 20% following an interaction quench from $\Lambda = \lambda_0(N-1) = 0.09$ to 0.18 at $t = 0$. Compare to Fig. 4. It is found that the results with $M = 3$ accurately describe the physics and the results with $M = 6$ and $M = 10$ orbitals lie atop each other. The quantities shown are dimensionless.

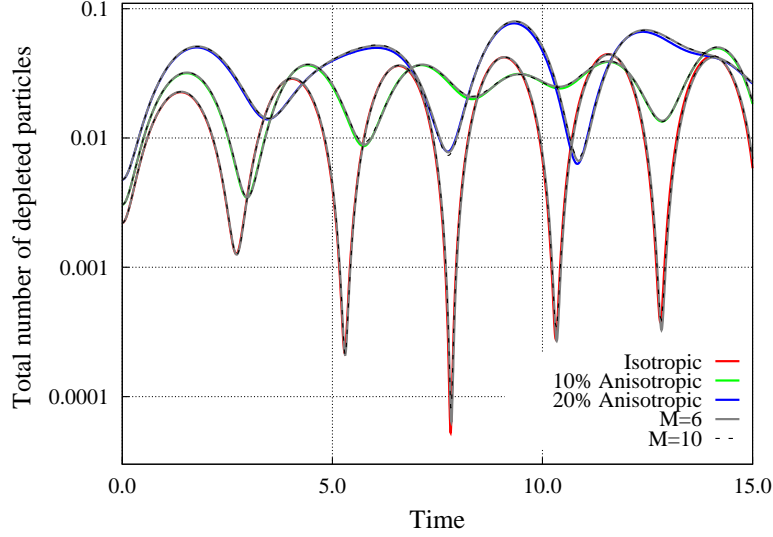


FIG. 7. (Color online) Convergence of the total number of depleted particles with the number of time-adaptive orbitals M used in the MCTDHB computations for systems consisting of $N = 10$ bosons following an interaction quench from $\Lambda = \lambda_0(N - 1) = 0.09$ to 0.18 at $t = 0$, see Fig. 6. It is found that the results with $M = 3$ accurately describe the physics and the results with $M = 6$ and $M = 10$ orbitals lie atop each other. Compare to Fig. 5. The quantities shown are dimensionless.

also see in this context [100]. It is found that the results are nicely converged.

-
- [1] C. Cohen-Tannoudji, B. Diu, and F. Laloë, *Quantum Mechanics*, Vol. 1 (Wiley, New York, 1977).
 - [2] M. H. Anderson, J. R. Ensher, M. R. Matthews, C. E. Wieman, and E. A. Cornell, Observation of Bose-Einstein Condensation in a Dilute Atomic Vapor, *Science* **269**, 198 (1995).
 - [3] C. C. Bradley, C. A. Sackett, J. J. Tollett, and R. G. Hulet, Evidence of Bose-Einstein Condensation in an Atomic Gas with Attractive Interactions, *Phys. Rev. Lett.* **75**, 1687 (1995).
 - [4] K. B. Davis, M.-O. Mewes, M. R. Andrews, N. J. van Druten, D. S. Durfee, D. M. Kurn, and W. Ketterle, Bose-Einstein Condensation in a Gas of Sodium Atoms, *Phys. Rev. Lett.* **75**, 3969 (1995).

- [5] E. A. Cornell and C. E. Wieman, Nobel Lecture: Bose-Einstein condensation in a dilute gas, the first 70 years and some recent experiments, *Rev. Mod. Phys.* **74**, 875 (2002).
- [6] W. Ketterle, Nobel lecture: When atoms behave as waves: Bose-Einstein condensation and the atom laser, *Rev. Mod. Phys.* **74**, 1131 (2002).
- [7] F. Dalfovo, S. Giorgini, L. P. Pitaevskii, and S. Stringari, Theory of Bose-Einstein condensation in trapped gases, *Rev. Mod. Phys.* **71**, 463 (1999).
- [8] A. J. Leggett, Bose-Einstein condensation in the alkali gases: Some fundamental concepts, *Rev. Mod. Phys.* **73**, 307 (2001).
- [9] I. Bloch, J. Dalibard, and W. Zwerger, Many-body physics with ultracold gases, *Rev. Mod. Phys.* **80**, 885 (2008).
- [10] V. I. Yukalov, Basics of Bose-Einstein condensation, *Phys. Part. Nucl.* **42**, 460 (2011).
- [11] L. Pitaevskii and S. Stringari, *Bose-Einstein Condensation* (Oxford University Press, Oxford, 2003).
- [12] A. J. Leggett, *Quantum Liquids: Bose condensation and Cooper pairing in condensed matter systems* (Oxford University Press, Oxford, 2006).
- [13] C. J. Pethick and H. Smith, *Bose-Einstein Condensation in Dilute Gases*, 2nd ed. (Cambridge University Press, Cambridge, England, 2008).
- [14] E. H. Lieb, R. Seiringer, and J. Yngvason, Bosons in a trap: A rigorous derivation of the Gross-Pitaevskii energy functional, *Phys. Rev. A* **61**, 043602 (2000).
- [15] E. H. Lieb and R. Seiringer, Proof of Bose-Einstein Condensation for Dilute Trapped Gases, *Phys. Rev. Lett.* **88**, 170409 (2002).
- [16] L. Erdős, B. Schlein, and H.-T. Yau, Rigorous Derivation of the Gross-Pitaevskii Equation, *Phys. Rev. Lett.* **98**, 040404 (2007).
- [17] L. Erdős, B. Schlein, and H.-T. Yau, Derivation of the cubic non-linear Schrödinger equation from quantum dynamics of many-body systems, *Invent. Math.* **167**, 515 (2007).
- [18] Y. Castin and R. Dum, Low-temperature Bose-Einstein condensates in time-dependent traps: Beyond the U(1) symmetry breaking approach, *Phys. Rev. A* **57**, 3008 (1998).
- [19] L. S. Cederbaum, Exact many-body wave function and properties of trapped bosons in the infinite-particle limit, *Phys. Rev. A* **96**, 013615 (2017).
- [20] S. Klaiman and O. E. Alon, Variance as a sensitive probe of correlations, *Phys. Rev. A* **91**, 063613 (2015).

- [21] S. Klaiman, A. I. Streltsov, and O. E. Alon, Uncertainty product of an out-of-equilibrium many-particle system, *Phys. Rev. A* **93**, 023605 (2016).
- [22] T. Vaughan, P. Drummond, and G. Leuchs, Quantum limits to center-of-mass measurements, *Phys. Rev. A* **75**, 033617 (2007).
- [23] Y.-J. Chen, S. Pabst, Z. Li, O. Vendrell, and R. Santra, Dynamics of fluctuations in a quantum system, *Phys. Rev. A* **89**, 052113 (2014).
- [24] S. Klaiman, A. I. Streltsov, and O. E. Alon, Solvable model of a trapped mixture of Bose-Einstein condensates, *Chem. Phys.* **482**, 362 (2017).
- [25] S. Klaiman, A. I. Streltsov, and O. E. Alon, Solvable Model of a Generic Trapped Mixture of Interacting Bosons: Many-Body and Mean-Field Properties at the Infinite-Particle Limit, arXiv:1708.00687v1 [cond-mat.quant-gas].
- [26] S. Klaiman and L. S. Cederbaum, Overlap of exact and Gross-Pitaevskii wave functions in Bose-Einstein condensates of dilute gases, *Phys. Rev. A* **94**, 063648 (2016).
- [27] S. Klaiman, A. I. Streltsov, and O. E. Alon, Uncertainty product of an out-of-equilibrium Bose-Einstein condensates, *J. Phys.: Conf. Ser.* **826**, 012020 (2017).
- [28] P.-O. Löwdin, Quantum Theory of Many-Particle Systems. I. Physical Interpretations by Means of Density Matrices, Natural Spin-Orbitals, and Convergence Problems in the Method of Configurational Interaction, *Phys. Rev.* **97**, 1474 (1955).
- [29] A. J. Coleman and V. I. Yukalov, *Reduced Density Matrices: Coulson's Challenge*, Lectures Notes in Chemistry Vol. 72 (Springer, Berlin, 2000).
- [30] *Reduced-Density-Matrix Mechanics: with Application to Many-Electron Atoms and Molecules*, edited by D. A. Mazziotti, Advances in Chemical Physics Vol. 134 (Wiley, New York, 2007).
- [31] K. Sakmann, A. I. Streltsov, O. E. Alon, and L. S. Cederbaum, Reduced density matrices and coherence of trapped interacting bosons, *Phys. Rev. A* **78**, 023615 (2008).
- [32] O. Penrose and L. Onsager, Bose-Einstein Condensation and Liquid Helium, *Phys. Rev.* **104**, 576 (1956).
- [33] R. L. Hall, Some exact solutions to the translation-invariant N-body problem, *J. Phys. A* **11**, 1227 (1978).
- [34] R. L. Hall, Exact solutions of Schrödinger's equation for translation-invariant harmonic matter, *J. Phys. A* **11**, 1235 (1978).

- [35] L. Cohen and C. Lee, Exact reduced density matrices for a model problem, *J. Math. Phys.* **26**, 3105 (1985).
- [36] M. S. Osadchii and V. V. Murakhtanov, The System of Harmonically Interacting Particles: An Exact Solution of the Quantum-Mechanical Problem, *Int. J. Quant. Chem.* **39**, 173 (1991).
- [37] M. A. Załuska-Kotur, M. Gajda, A. Orłowski, and J. Mostowski, Soluble model of many interacting quantum particles in a trap, *Phys. Rev. A* **61**, 033613 (2000).
- [38] J. Yan, Harmonic Interaction Model and Its Applications in Bose-Einstein Condensation, *J. Stat. Phys.* **113**, 623 (2003).
- [39] M. Gajda, Criterion for Bose-Einstein condensation in a harmonic trap in the case with attractive interactions, *Phys. Rev. A* **73**, 023603 (2006).
- [40] J. R. Armstrong, N. T. Zinner, D. V. Fedorov, and A. S. Jensen, Analytic harmonic approach to the N-body problem, *J. Phys. B* **44** 055303, (2011).
- [41] J. R. Armstrong, N. T. Zinner, D. V. Fedorov, and A. S. Jensen, Virial expansion coefficients in the harmonic approximation, *Phys. Rev. E* **86**, 021115 (2012).
- [42] C. Schilling, Natural orbitals and occupation numbers for harmonium: Fermions versus bosons, *Phys. Rev. A* **88**, 042105 (2013).
- [43] C. L. Benavides-Riveros, I. V. Toranzo, and J. S. Dehesa, Entanglement in N-harmonium: bosons and fermions, *J. Phys. B* **47**, 195503 (2014).
- [44] P. A. Bouvrie, A. P. Majtey, M. C. Tichy, J. S. Dehesa, and A. R. Plastino, Entanglement and the Born-Oppenheimer approximation in an exactly solvable quantum many-body system, *Eur. Phys. J. D* **68**, 346 (2014).
- [45] J. R. Armstrong, A. G. Volosniev, D. V. Fedorov, A. S. Jensen, and N. T. Zinner, Analytic solutions of topologically disjoint systems, *J. Phys. A* **48**, 085301 (2015).
- [46] C. Schilling and R. Schilling, Number-parity effect for confined fermions in one dimension, *Phys. Rev.* **93**, 021601(R) (2016).
- [47] O. E. Alon, Solvable model of a generic trapped mixture of interacting bosons: reduced density matrices and proof of BoseEinstein condensation, *J. Phys. A* **50**, 295002 (2017).
- [48] A. I. Streltsov, O. E. Alon, and L. S. Cederbaum, Role of Excited States in the Splitting of a Trapped Interacting Bose-Einstein Condensate by a Time-Dependent Barrier, *Phys. Rev. Lett.* **99**, 030402 (2007).

- [49] O. E. Alon, A. I. Streltsov, and L. S. Cederbaum, Multiconfigurational time-dependent Hartree method for bosons: Many-body dynamics of bosonic systems, *Phys. Rev. A* **77**, 033613 (2008).
- [50] K. Sakmann, A. I. Streltsov, O. E. Alon, and L. S. Cederbaum, Exact Quantum Dynamics of a Bosonic Josephson Junction, *Phys. Rev. Lett.* **103**, 220601 (2009).
- [51] J. Grond, J. Schmiedmayer, and U. Hohenester, Optimizing number squeezing when splitting a mesoscopic condensate, *Phys. Rev. A* **79**, 021603(R) (2009).
- [52] J. Grond, T. Betz, U. Hohenester, N. J. Mauser, J. Schmiedmayer, and T. Schumm, The Shapiro effect in atomchip-based bosonic Josephson junctions, *New J. Phys.* **13**, 065026 (2011).
- [53] I. Březinová, Axel U. J. Lode, Alexej I. Streltsov, Ofir E. Alon, Lorenz S. Cederbaum, and J. Burgdörfer, Wave chaos as signature for depletion of a Bose-Einstein condensate, *Phys. Rev. A* **86**, 013630 (2012).
- [54] M. Heimsoth, D. Hochstuhl, C. E. Creffield, L. D. Carr, and F. Sols, Effective Josephson dynamics in resonantly driven Bose-Einstein condensates, *New J. Phys.* **15**, 103006 (2013).
- [55] S. Klaiman, A. U. J. Lode, A. I. Streltsov, L. S. Cederbaum, and O. E. Alon, Breaking the resilience of a two-dimensional Bose-Einstein condensate to fragmentation, *Phys. Rev. A* **90**, 043620 (2014).
- [56] S. I. Mistakidis, L. Cao, and P. Schmelcher, Negative-quench-induced excitation dynamics for ultracold bosons in one-dimensional lattices, *Phys. Rev. A* **91**, 033611 (2015).
- [57] S. Krönke and P. Schmelcher, Many-body processes in black and gray matter-wave solitons, *Phys. Rev. A* **91**, 053614 (2015).
- [58] U. R. Fischer, A. U. J. Lode, and B. Chatterjee, Condensate fragmentation as a sensitive measure of the quantum many-body behavior of bosons with long-range interactions, *Phys. Rev. A* **91**, 063621 (2015).
- [59] S. Krönke and P. Schmelcher, Two-body correlations and natural-orbital tomography in ultracold bosonic systems of definite parity, *Phys. Rev. A* **92**, 023631 (2015).
- [60] R. Beinke, S. Klaiman, L. S. Cederbaum, A. I. Streltsov, and O. E. Alon, Many-body tunneling dynamics of Bose-Einstein condensates and vortex states in two spatial dimensions, *Phys. Rev. A* **92**, 043627 (2015).

- [61] S. I. Mistakidis, T. Wulf, A. Negretti, and P. Schmelcher, Resonant quantum dynamics of few ultracold bosons in periodically driven finite lattices, *J. Phys. B* **48**, 244004 (2015).
- [62] I. Brouzos, A. I. Streltsov, A. Negretti, R. S. Said, T. Caneva, S. Montangero, and T. Calarco, Quantum Speed Limit and Optimal Control of Many-Boson Dynamics, *Phys. Rev. A* **92**, 062110 (2015).
- [63] K. Sakmann and M. Kasevich, Single shot simulations of dynamic quantum many-body systems, *Nat. Phys.* **12**, 451 (2016).
- [64] A. U. J. Lode, Multiconfigurational time-dependent Hartree method for bosons with internal degrees of freedom: Theory and composite fragmentation of multicomponent Bose-Einstein condensates, *Phys. Rev. A* **93**, 063601 (2016).
- [65] S. E. Weiner, M. C. Tsatsos, L. S. Cederbaum, and A. U. J. Lode, Phantom vortices: hidden angular momentum in ultracold dilute Bose-Einstein condensates, *Sci Rep.* **7**, 40122 (2017).
- [66] J. G. Cosme, M. F. Andersen, and J. Brand, Interaction blockade for bosons in an asymmetric double well, *Phys. Rev. A* **96**, 013616 (2017).
- [67] O. V. Marchukov and U. R. Fischer, Phase-fluctuating condensates are fragmented: An experimental benchmark for self-consistent quantum many-body calculations, *arXiv:1701.06821v2 [cond-mat.quant-gas]*.
- [68] K. Sakmann, *Many-Body Schrödinger Dynamics of Bose-Einstein Condensates*, Springer Theses (Springer, Heidelberg, 2011).
- [69] *Quantum Gases: Finite Temperature and Non-Equilibrium Dynamics*, edited by N. P. Proukakis, S. A. Gardiner, M. J. Davis, and M. H. Szymanska, Cold Atoms Series Vol. 1 (Imperial College Press, London, 2013).
- [70] A. U. J. Lode, *Tunneling Dynamics in Open Ultracold Bosonic Systems*, Springer Theses (Springer, Heidelberg, 2015).
- [71] A. U. J. Lode, K. Sakmann, O. E. Alon, L. S. Cederbaum, and A. I. Streltsov, Numerically exact quantum dynamics of bosons with time-dependent interactions of harmonic type, *Phys. Rev. A* **86**, 063606 (2012).
- [72] E. Fasshauer and A. U. J. Lode, Multiconfigurational time-dependent Hartree method for fermions: Implementation, exactness, and few-fermion tunneling to open space, *Phys. Rev. A* **93**, 033635 (2016).

- [73] H.-D. Meyer, U. Manthe, and L. S. Cederbaum, The multi-configurational time-dependent Hartree approach, *Chem. Phys. Lett.* **165**, 73 (1990).
- [74] U. Manthe, H.-D. Meyer, and L. S. Cederbaum, Wave-packet dynamics within the multiconfiguration Hartree framework: General aspects and application to NOCl, *J. Chem. Phys.* **97**, 3199 (1992).
- [75] M. H. Beck, A. Jäckle, G. A. Worth, and H. D. Meyer, The multiconfiguration time-dependent Hartree (MCTDH) method: a highly efficient algorithm for propagating wavepackets, *Phys. Rep.* **324**, 1 (2000).
- [76] *Multidimensional Quantum Dynamics: MCTDH Theory and Applications*, edited by H.-D. Meyer, F. Gatti, and G. A. Worth (Wiley-VCH, Weinheim, 2009).
- [77] R. W. Spekkens and J. E. Sipe, Spatial fragmentation of a Bose-Einstein condensate in a double-well potential, *Phys. Rev. A* **59**, 3868 (1999).
- [78] A. I. Streltsov, L. S. Cederbaum, and N. Moiseyev, Ground-state fragmentation of repulsive Bose-Einstein condensates in double-trap potentials, *Phys. Rev. A* **70**, 053607 (2004).
- [79] O. E. Alon and L. S. Cederbaum, Pathway from Condensation via Fragmentation to Fermionization of Cold Bosonic Systems, *Phys. Rev. Lett.* **95**, 140402 (2005).
- [80] S. Zöllner, H.-D. Meyer, and P. Schmelcher, Correlations in ultracold trapped few-boson systems: Transition from condensation to fermionization, *Phys. Rev. A* **74**, 063611 (2006).
- [81] A. I. Streltsov, O. E. Alon, and L. S. Cederbaum, General variational many-body theory with complete self-consistency for trapped bosonic systems, *Phys. Rev. A* **73**, 063626 (2006).
- [82] P. Nozières and D. Saint James, Particle vs. pair condensation in attractive Bose liquids, *J. Phys. (Paris)* **43**, 1133 (1982).
- [83] P. Nozières, in *Bose-Einstein Condensation*, edited by A. Griffin, D. W. Snoke, and S. Stringari (Cambridge University Press, Cambridge, 1996), p. 15.
- [84] E. J. Mueller, T.-L. Ho, M. Ueda, and G. Baym, Fragmentation of Bose-Einstein condensates, *Phys. Rev. A* **74**, 033612 (2006).
- [85] U. R. Fischer and P. Bader, Interacting trapped bosons yield fragmented condensate states in low dimensions, *Phys. Rev. A* **82**, 013607 (2010).
- [86] Q. Zhou and X. Cui, Fate of a Bose-Einstein Condensate in the Presence of Spin-Orbit Coupling, *Phys. Rev. Lett.* **110**, 140407 (2013).

- [87] Y. Kawaguchi, Goldstone-mode instability leading to fragmentation in a spinor Bose-Einstein condensate, *Phys. Rev. A* **89**, 033627 (2014).
- [88] S.-W. Song, Y.-C. Zhang, H. Zhao, X. Wang, and W.-M. Liu, Fragmentation of spin-orbit-coupled spinor Bose-Einstein condensates, *Phys. Rev. A* **89**, 063613 (2014).
- [89] H. H. Jen and S.-K. Yip, Fragmented many-body states of a spin-2 Bose gas, *Phys. Rev. A* **91**, 063603 (2015).
- [90] A. R. Kolovsky, Bogoliubov depletion of the fragmented condensate in the bosonic flux ladder, *Phys. Rev. A* **95**, 033622 (2017).
- [91] P. Bader and U. R. Fischer, Fragmented Many-Body Ground States for Scalar Bosons in a Single Trap, *Phys. Rev. Lett.* **103**, 060402 (2009).
- [92] A. I. Streltsov, Quantum systems of ultracold bosons with customized interparticle interactions, *Phys. Rev. A* **88**, 041602(R) (2013).
- [93] M.-K. Kang and U. R. Fischer, Revealing Single-Trap Condensate Fragmentation by Measuring Density-Density Correlations after Time of Flight, *Phys. Rev. Lett.* **113**, 140404 (2014).
- [94] O. I. Streltsova, O. E. Alon, L. S. Cederbaum, and A. I. Streltsov, Generic regimes of quantum many-body dynamics of trapped bosonic systems with strong repulsive interactions, *Phys. Rev. A* **89**, 061602(R) (2014).
- [95] U. R. Fischer and M.-K. Kang, Photonic Cat States from Strongly Interacting Matter Waves, *Phys. Rev. Lett.* **115**, 260404 (2015).
- [96] S. Bauch, K. Balzer, C. Henning, and M. Bonitz, Quantum breathing mode of trapped bosons and fermions at arbitrary coupling, *Phys. Rev. B* **80**, 054515 (2009).
- [97] R. Schmitz, S. Krönke, L. Cao, and P. Schmelcher, Quantum breathing dynamics of ultracold bosons in one-dimensional harmonic traps: Unraveling the pathway from few- to many-body systems, *Phys. Rev. A* **88** 043601 (2013).
- [98] A. I. Streltsov and O. I. Streltsova, MCTDHB-Lab, version 1.5, 2015, <http://www.mctdhlb-lab.com>.
- [99] A. I. Streltsov, L. S. Cederbaum, O. E. Alon, K. Sakmann, A. U. J. Lode, J. Grond, O. I. Streltsova, S. Klaiman, and R. Beinke, The Multiconfigurational Time-Dependent Hartree for Bosons Package, version 3.x, <http://mctdhlb.org>, Heidelberg/Kassel (2006-present).
- [100] J. G. Cosme, C. Weiss, and J. Brand, Center-of-mass motion as a sensitive convergence test for variational multimode quantum dynamics, *Phys. Rev. A* **94**, 043603 (2016).